# A combined chemical/size fractionation approach to study winter/summer variations, ageing and source strength of atmospheric particles

S. Canepari[1]*, M.L. Astolfi[1], M. Catrambone[2], D. Frasca[1,2], M. Marcoccia[1], F. Marcovecchio[2], L. Massimi[1], E. Rantica[2], C. Perrino[2]

[1]Department of Chemistry, Sapienza University of Rome, P.le Aldo Moro, 5, Rome, 00185, Italy

[2]C.N.R. Institute of Atmospheric Pollution Research,
Via Salaria, Km 29,300, Monterotondo St. (Rome), 00015, Italy

*Corresponding author. E-mail: silvia.canepari@uniroma1.it Tel.: +39 0649913343

ABSTRACT

We studied the size distribution of ions ($Cl^-$, $NO_3^-$, $SO_4^{=}$, $Na^+$, $NH_4^+$, $K^+$, $Mg^{++}$, $Ca^{++}$) and elements (As, Ba, Cd, Co, Cs, Cu, Fe, Li, Mn, Ni, Pb, Rb, Sb, Se, Sn, Sr, Ti, Tl, V, Zn) during the winter and summer seasons of seven consecutive years (2008 – 2014) in an area of the Po Valley (Northern Italy) characterised by industrial, agricultural and urban settings. The study included the collection and analysis of 41 series of size-segregated samples (MOUDI sampler, 10 stages, cut sizes from 0.18 to 18 μm). Ions were analysed by ion chromatography; elemental analysis was carried out by ICP-MS, by applying a chemical fractionation method able to increase the selectivity of PM source tracers.

Our results indicate that important winter/summer variations occurred in both the concentration and size distribution of most PM components. These variations were explained in terms of variations in the strength of the prevailing sources of each component.

The contribution of biomass burning for domestic heating was highlighted by the well-known tracer $K^+$ but also by the soluble fraction of Rb, Cs and Li. Biomass burning contribution to atmospheric PM was mostly contained in the fine fraction, with a broad size-distribution from 0.18 to 1.8 μm. This source also appreciably increased the concentration of other elements in fine PM (As, Cd, Co, Mn, Pb, Sb, Sn).

A few PM components (tracers of sea-spray, brake lining and some industries) did not show marked seasonal variations in concentration and size distribution. However, during winter, for brake lining and industry tracers we observed an upward shift in the dimension of fine particles and a downward shift in the dimension of coarse particles, due to the ageing of the air masses.

KEY WORDS
Size distribution; MOUDI impactor; elemental composition; source tracers; biomass burning

## INTRODUCTION

It is well known that the size distribution of atmospheric particles strictly depends on their sources and on the atmospheric processes they undergo during their lifetime. The size distribution of atmospheric particulate matter (PM) also defines the effects it produces on human health and on the ecosystem (EPA, 2004). Consequently, the study of the size distribution of the chemical components of PM can be of great help in providing valuable information for the source apportionment, the study of particle ageing processes and the identification of health and climate effects (Canepari et al., 2008; Cassee et al., 2013; Liu et al., 2015; Gao et al., 2016; Bernardoni et al., 2017).

In the case of elements, their chemical fractionation constitutes a further, precious source of information for evaluating the strength of PM sources. The independent measurement of elemental fractions characterised by different solubility, in fact, ensures a better accuracy in the use of tracers for the identification of PM sources (Canepari et al., 2009, 2014; Wang et al., 2015; Arhami et al., 2017).

Even more powerful is the combination of chemical and size fractionation. Previous scientific works (Canepari et al., 2008, 2010; Wang et al., 2016; Barbaro et al., 2019) showed the potential of this approach, particularly suitable for geographical areas characterized by frequent and long-lasting atmospheric stabilities, where co-variation of pollutants is frequently observed. This combination of chemical and size fractionation is also of great help in tricky situations where it is necessary to identify and evaluate the impact of different emission sources that share many chemical PM components.

Many literature studies concern the size distribution of PM (Salma et al., 2005; Maudlin et al., 2015; Nirmalkar et al., 2016; Castro et al., 2018; Ma et al., 2019) and the seasonal variations of $PM_{10}$ and/or $PM_{2.5}$ concentration (Perrino et al., 2014; Hwang et al., 2018). However, very few papers examine the seasonal variations in concentration and composition of size-segregated PM samples (Chrysikou and Samara, 2009; Taiwo et al., 2014; Zhang et al., 2018).

In this work we applied the chemical/size fractionation method to 14 sampling campaigns carried out in the Po Valley during winter and summer of seven consecutive years (2008 – 2014). PM collection was carried out by using 10-stage MOUDI impactors. Size-segregated samples were analysed for PM mass, ions, extracted and residual fractions of elements.

The Po Valley is a geographical area sited in Northern Italy, characterised by a relevant impact due to urban areas, industrial facilities, agricultural activity and breeding farms. This area may be regarded as a challenging open-air laboratory, due to frequent, long-lasting and intense atmospheric

stability periods that cause fast worsening of air quality, formation of secondary species and relevant ageing of the air masses (Marcazzan et al., 2002; Pernigotti et al., 2012; Bigi and Ghermandi, 2014; Perrino et al., 2014, 2016). This area is thus an ideal training ground to check the performance of the chemical/dimensional fractionation approach.

## EXPERIMENTAL

Sampling was carried out in the vicinity of Ferrara, a city of about 130.000 inhabitants located in the eastern Po Valley, in Northern Italy. In the study area there are several PM sources: a highway, running at about 0.4 Km from the main sampling site, a major industrial site including a power plant, a urban incinerator and many small and medium size enterprises, located at about 2.5 Km, the city, at about 5 Km.

The study was carried out in one, two or three sites, according to the period. The main site, where all the 14 sampling campaigns were carried out, was a residential area located in the hamlet of Cassana (site C; Google co-ordinates: 44°50'54.95"N, 11°33'40.36"E). A site located inside the industrial area was added during the period 2011 – 2014 (site A; Google co-ordinates: 44°51'26.26"N, 11°33'36.90"E). A rural site, located as far as feasible from the main emission sources, was added during the period 2011 – 2012 (site B; Google co-ordinates: 44°49'31.53"N, 11°32'55.01"E). The location of three sampling sites in the study area is shown in Supplementary Material S1. Concentration and chemical composition of $PM_{10}$ and $PM_{2.5}$, elemental solubility and strength of the main PM sources at the three sampling sites were widely described in previous papers (Canepari et al., 2014; Farao et al., 2014; Perrino et al., 2014). As shown in these papers, the three sites, which are a few kilometers away from each other, can be considered as equivalent in terms of PM concentration and composition. This spatial homogeneity of the air masses is a peculiar feature of the Po Valley, due to the frequent very low mixing of the atmosphere. An interesting consequence of this feature is that the results obtained in individual monitoring sites may be considered as representative of a wide area.

The study was carried out during the winter (January-February) and the summer (June) of each year from 2008 to 2014, for a total of 14 periods. Each sampling campaign lasted for 3 or 4 weeks and was carried out simultaneously in one, two or three of the above sites. The inclusion of the additional sites strengthened the reliability of the dataset. The duration of each sampling was 2 or 3 weeks. In some cases, two sequential samplings per period were carried out. A total of 41 series of samples were collected during the whole study. Details about the sampling periods and sites are reported in Table I.

Size-segregated sampling was carried out by using three Micro-Orifice Uniform-Deposit Impactors (MOUDI mod. 110-R and 120-R, MSP Co., U.S.A.) operating at the flow rate of 30 L $min^{-1}$ and having ten collection stages (cut-sizes of 0.18, 0.32, 0.56, 1.0, 1.8, 3.2, 5.6, 10 and 18 µm in aerodynamic diameter). Sampling flow rate was daily adjusted to keep its variations within 5%. The impactors were equipped with Teflon membrane filters (TEFLO, 47 mm, 2.0 micron pore size, PALL Life Sciences). The performance of the three impactors had been previously compared during a preliminary campaign, in which they were run simultaneously for 3 weeks and analysed for ions. The sampling was carried out during the autumn of 2007 in a periurban site close to Rome. The relative standard deviation of the three replicates for each stage, which includes also the uncertainty of the analytical procedure, was always lower than 25%. The results are reported in Supplementary Material S2.

It is worth noting that long-duration samplings carried out by using cascade impactors might undergo sampling artefacts. Among these, loss by evaporation of ammonium nitrate and chloride may lead to depletion of these ions. However, to our knowledge, there are no solid and recognized methods to correct the data for this artefact. Furthermore, particle bouncing-off phenomena may be responsible for a modification of the original size distribution of atmospheric particles (EPA, 2004). However, Teflon filters are generally considered as a suitable sampling material from this point of view, able to minimize the bouncing-off (Giorio et al., 2013). Moreover, none of these phenomena change the chemical composition of the individual particles and the co-variation of source tracers is nevertheless maintained.

Table I: Schedule and location of the samplings carried out during the study.

| Year | Season | Monitoring period | Site | Number and duration of samplings | Total number of samples |
|---|---|---|---|---|---|
| 2008 | winter | 15/01 – 12/02 | C | 2 x 2 weeks | 2 |
| 2008 | summer | 29/05 – 12/06 | C | 1 x 2 weeks | 1 |
| 2009 | winter | 08/01 – 05/02 | C | 2 x 2 weeks | 2 |
| 2009 | summer | 27/05 – 10/06 | C | 1 x 2 weeks | 1 |
| 2010 | winter | 12/01 – 09/02 | C | 2 x 2 weeks | 2 |
| 2010 | summer | 02/06 – 16/06 | C | 1 x 2 weeks | 1 |
| 2011 | winter | 11/01 – 07/02 | A, B, C | 2 x 2 weeks | 6 |
| 2011 | summer | 31/05 – 28/06 | A, B, C | 2 x 2 weeks | 6 |
| 2012 | winter | 12/01 – 09/02 | A, B, C | 2 x 2 weeks | 6 |

| | | | | | |
|---|---|---|---|---|---|
| 2012 | summer | 30/05 – 27/05 | A, B, C | 2 x 2 weeks | 6 |
| 2013 | winter | 10/01 – 31/01 | A, C | 1 x 3 weeks | 2 |
| 2013 | summer | 30/05 – 20/06 | A, C | 1 x 3 weeks | 2 |
| 2014 | winter | 09/01 – 30/01 | A, C | 1 x 3 weeks | 2 |
| 2014 | summer | 05/06 – 26/06 | A, C | 1 x 3 weeks | 2 |

Mass concentration on the MOUDI stages was determined gravimetrically by using an automated microbalance (1 μg sensitivity, mod. ME5, Sartorius AG, Goettingen, Germany): Filters were equilibrated for two days at 20°C and 50% RH before and after the sampling..

For the analysis of ions and element on the same Teflon filter, the extraction was carried out in deionized water and the solution was first analyzed for ions ($Cl^-$, $NO_3^-$, $SO_4^=$, $Na^+$, $NH_4^+$, $K^+$, $Mg^{++}$, $Ca^{++}$) by ion chromatography (ICS1000, Dionex Co., CA, U.S.A.); then acetate buffer ($CH_3COOH/CH_3COOK$ 0.01M; ph4.3) was added and the solution was filtered and analyzed for the extracted fraction of elements (As, Ba, Cd, Co, Cs, Cu, Fe, Li, Mn, Ni, Pb, Rb, Sb, Se, Sn, Sr, Ti, Tl, V, Zn) by inductively coupled plasma mass spectroscopy (ICP-MS, Bruker 820MS). Solid residual on both the sampling filter and the filtration filter was subjected to microwave-assisted acid digestion and analyzed by ICP-MS for the same elements (residual fraction). The procedure was previously optimized and fully validated and the relative repeatability for all the considered variables was found to below 10%; more details about the analytical performances are reported in Canepari et al. (2009b). Limits of Detection (LODs) were calculated as mean value of filter blanks (6 replicates) plus three times its standard deviation.

To obtain an easy comparison among the results and to reduce the effect of the variability in the environmental concentrations occurring during different sampling periods, the analytical results were treated as follows. For each PM component and for each MOUDI sample, the results obtained from the analysis of the ten stages were added up and each individual result was expressed as a per cent with respect to the sum. The per cent values obtained for each stage in all winter or summer samples were averaged to obtain a winter/summer mean percentage (and standard deviation). These mean per cent values (winter/summer average per cent distribution) were recalculated considering as reference value the highest one between the two sum values obtained for winter and for summer. This latter choice was aimed at visualising the seasonal differences in each graph.

## RESULTS AND DISCUSSION

In general, the mass concentration and chemical composition of atmospheric PM in the area of the Po Valley are spatially homogeneous, particularly during the winter season (Marcazzan et al., 2002; Canepari et al., 2014; Perrino et al., 2014). This characteristic was confirmed during the years 2011-2012 of our study, when the samplings were simultaneously carried out at sites A, B and C. As an example, in Figure 1 we report the size-segregated mass concentration measured at the three sites during the winter (upper panel) and the summer (lower panel) of 2012. The distance between the two furthest sites, A and C, is about 3.5 Km. The results obtained at the three sites were very similar, not only in terms of concentration but also as far as the size distribution is concerned. The results obtained from the whole study can be thus considered as representative of a wider area.

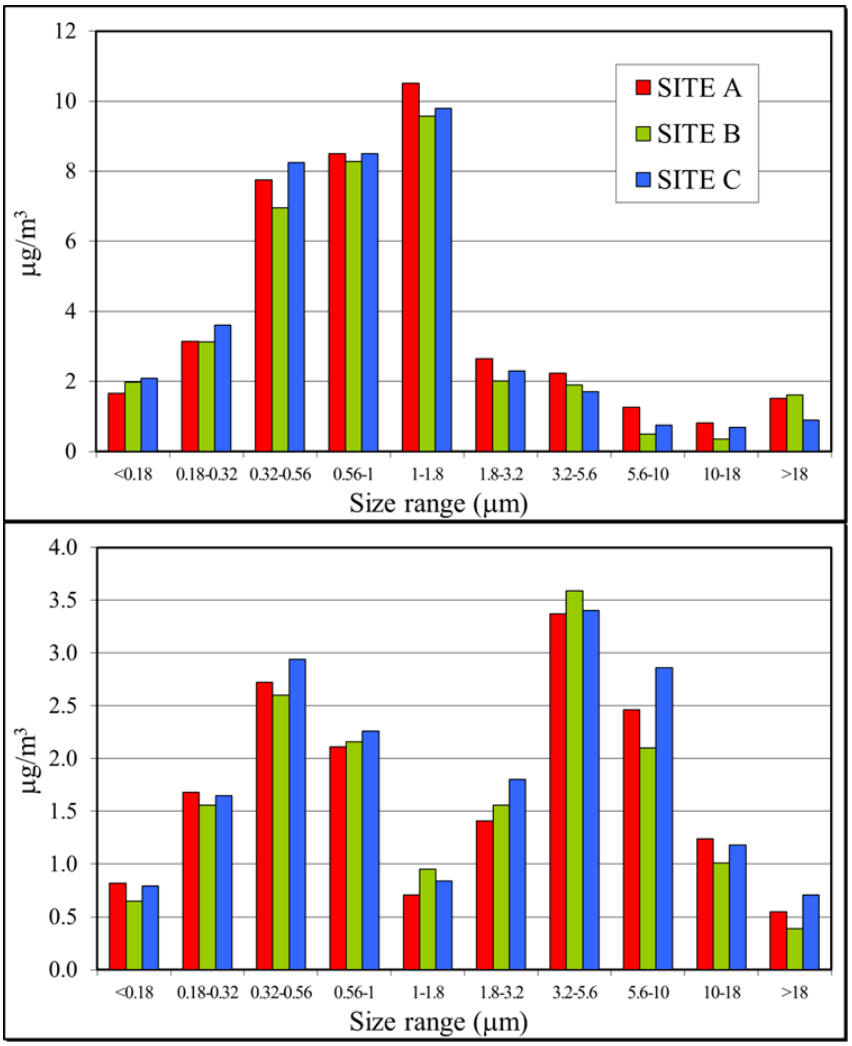


Figure 1: Size distribution of PM at the three sampling sites during the winter (upper panel) and the summer (lower panel) of 2012.

The data reported in Figure 1 also show that there are noteworthy seasonal differences in the concentration and size distribution of PM: during winter, concentration values were much higher

(about three times) than summer values and the size distribution showed a clear prevalence of the fine fraction, with maximum concentrations in the size range 1.0 – 1.8 μm. During summer, instead, the size distribution showed a bi-modal pattern, with a first maximum in the coarse fraction (size range 3.2 – 5.6 μm) and a second maximum in the fine fraction (0.32 – 0.56 μm).

These results are in agreement with the winter increase in the concentration of fine particles due to both the formation of secondary species in conditions of strong and long-lasting atmospheric stability (Marcazzan et al., 2002; Bigi and Ghermandi, 2014) and the switch-on of domestic heating, especially by biomass burning. Both mechanisms are responsible for the production of particles in the fine dimensional range. During the summer period, instead, the more efficient atmospheric mixing and the absence of domestic heating causes a decrease in the concentration of fine particles, while the aridity favours the re-suspension of soil particles, increasing the concentration of the coarse fraction of PM (Kulshrestha et al., 2009). It is worth noting that the summer concentration of PM in the coarse fraction widely exceeded the winter values.

The concentration of the considered PM components (ions, elements expressed as sum of the extracted and residual fractions) during all the sampling periods of the winter and summer campaigns are reported in Table II as mean and standard deviation of the sum of the ten MOUDI stages. The reported LODs refer to a sampling volume of 600 $m^3$ (2 weeks). In the case of elements, they were obtained as sum of the extracted and residual fractions.

An overview of the data shows that for some PM components the winter and summer concentrations were very different. Among ions, nitrate concentration exhibited a very high winter to summer ratio (W/S > 8) as during winter it was mainly in the form of ammonium nitrate, a secondary species deeply affected by the frequent conditions of strong atmospheric stability occurring in the area during the cold season. In the Po valley, ammonium nitrate may constitute up to 30% of the PM mass, often constituting the most abundant individual PM component. In other geographical areas, instead, secondary inorganic species are dominated by ammonium sulphate (Ma et al., 2019).

Significant seasonal differences (W/S > 3) were also shown by $K^+$, which is affected by biomass burning emission. For sulphate ion, the seasonal difference were smaller (W/S = 1.6), as during winter this species is affected by the influence of atmospheric stability and by the transport from Eastern Europe (Squizzato et al., 2012; Canepari et al., 2014), while the contribution due to photochemical formation of ammonium sulphate prevails during summer. Winter concentration of chloride exceeded summer values (W/S > 3) due to the contribution of ammonium chloride, which during winter adds to the contribution due to sea-salt. PM release from sea did not show clear seasonal differences in this area, as demonstrated also by $Na^+$ and $Mg^{++}$ values. For $Ca^{++}$, mainly contained in soil dust, winter concentration was generally lower than summer values (W/S = 0.7).

Table II: Detection Limit (LOD) on individual stages and total concentration (sum of the 10 stages) during the two seasons: mean value of all the results and standard deviation. Units are μg/m$^3$, for ions and ng/m$^3$ for elements.

| | Analytical technique | LOD | WINTER (N=22) | | SUMMER (N=19) | |
|---|---|---|---|---|---|---|
| | | | MEAN | ST. DEV. | MEAN | ST.DEV. |
| $Cl^-$ | IC | 0.0001 | 0.39 | 0.05 | 0.11 | 0.01 |
| $NO_3^-$ | IC | 0.0003 | 9.1 | 0.6 | 1.1 | 0.1 |
| $SO_4^=$ | IC | 0.0005 | 3.1 | 0.1 | 2.0 | 0.1 |
| $Na^+$ | IC | 0.0002 | 0.32 | 0.03 | 0.25 | 0.02 |
| $NH_4^+$ | IC | 0.0002 | 2.7 | 0.2 | 0.70 | 0.03 |
| $K^+$ | IC | 0.0003 | 0.32 | 0.02 | 0.094 | 0.005 |
| $Mg^{++}$ | IC | 0.0003 | 0.049 | 0.003 | 0.053 | 0.003 |
| $Ca^{++}$ | IC | 0.0008 | 0.52 | 0.03 | 0.38 | 0.02 |
| As | ICP-MS | 0.003 | 0.78 | 0.04 | 0.59 | 0.02 |
| Ba | ICP-MS | 0.005 | 3.5 | 0.2 | 3.2 | 0.1 |
| Cd | ICP-MS | 0.01 | 0.33 | 0.02 | 0.10 | 0.01 |
| Co | ICP-MS | 0.0005 | 0.11 | 0.01 | 0.080 | 0.009 |
| Cs | ICP-MS | 0.00005 | 0.037 | 0.003 | 0.026 | 0.002 |
| Cu | ICP-MS | 0.01 | 8.7 | 0.6 | 6.5 | 0.3 |
| Fe | ICP-MS | 0.3 | 170 | 8 | 159 | 10 |
| Li | ICP-MS | 0.0005 | 0.14 | 0.01 | 0.24 | 0.01 |
| Mn | ICP-MS | 0.015 | 7.9 | 0.4 | 6.3 | 0.3 |
| Ni | ICP-MS | 0.005 | 2.5 | 0.2 | 3.0 | 0.5 |
| Pb | ICP-MS | 0.005 | 8.6 | 0.4 | 2.7 | 0.1 |
| Rb | ICP-MS | 0.005 | 1.4 | 0.1 | 1.6 | 0.1 |
| Sb | ICP-MS | 0.001 | 1.5 | 0.1 | 0.83 | 0.04 |
| Se | ICP-MS | 0.001 | 0.98 | 0.10 | 1.0 | 0.1 |
| Sn | ICP-MS | 0.001 | 2.1 | 0.1 | 1.0 | 0.1 |
| Sr | ICP-MS | 0.03 | 1.4 | 0.1 | 1.4 | 0.1 |
| Ti | ICP-MS | 0.005 | 1.8 | 0.1 | 3.5 | 0.2 |
| Tl | ICP-MS | 0.00005 | 0.028 | 0.002 | 0.024 | 0.001 |
| V | ICP-MS | 0.01 | 1.2 | 0.1 | 1.8 | 0.1 |
| Zn | ICP-MS | 0.5 | 57 | 4 | 39 | 4 |

Among elements, considerable differences between winter and summer were recorded for Cd, Pb (W/S > 3) and, at a less extent, Sb and Sn (W/S > 2). For those elements, winter increase could be due to the switch on of a typical seasonal source (domestic heating). W/S values below one were recorded for Li and Ti (W/S ≈ 0.5), elements that are typically contained in soil dust, more efficiently re-suspended during the warm, dry months.

Table III reports the solubility percentage of the elements, expressed as mean and standard deviation and referred to the sum of the ten MOUDI stages. In general, each element showed a typical solubility value. For example, Fe and Ti were found almost exclusively as insoluble species, while Cd, Rb, Tl and V were mostly in the extracted fraction. The other elements were distributed between the two solubility fractions. It is interesting to note that in some cases (e.g.: Cs and Li) there were significant seasonal variations in the solubility percentage, pointing at significant seasonal changes in the strength of the main sources of these elements.

Table III: Solubility percentage of the elements during the two seasons: mean value and standard deviation of all the results.

| | WINTER (N=22) | | SUMMER (N=19) | |
|---|---|---|---|---|
| | MEAN | ST.DEV. | MEAN | ST.DEV. |
| As | 77 | 6 | 62 | 15 |
| Ba | 51 | 9 | 33 | 11 |
| Cd | 81 | 4 | 77 | 11 |
| Co | 35 | 9 | 36 | 15 |
| Cs | 72 | 8 | 33 | 15 |
| Cu | 47 | 10 | 33 | 8 |
| Fe | 12 | 3 | 9 | 3 |
| Li | 63 | 12 | 23 | 13 |
| Mn | 58 | 9 | 53 | 9 |
| Ni | 31 | 9 | 30 | 13 |
| Pb | 35 | 6 | 43 | 8 |
| Rb | 93 | 2 | 77 | 12 |
| Sb | 62 | 8 | 52 | 5 |
| Se | 74 | 21 | 52 | 14 |
| Sn | 23 | 7 | 21 | 5 |
| Sr | 55 | 7 | 66 | 10 |

| | | | | |
|---|---|---|---|---|
| Ti | 6 | 2 | 3 | 2 |
| Tl | 89 | 5 | 91 | 11 |
| V | 70 | 12 | 72 | 12 |
| Zn | 55 | 17 | 50 | 12 |

The size distribution of the eight considered ions during the winter and the summer periods are reported in Figure 2 as seasonal mean and standard deviation. All the values were normalized as explained in the Experimental Section.

The size distributions of $Na^{+}$ and $Mg^{++}$ were very similar and unimodal, with maximum values in the range 3.2 – 5.6 μm, during both winter and summer. The prevalence of the coarse fraction is in agreement with the main source of these ions, from the sea. During winter, the same distribution in the coarse fraction was found for chloride; this ion, however, showed a bimodal distribution with a second maximum in the range 1-1.8 μm, due to ammonium chloride. During summer, instead, the concentration of coarse chloride was lower, probably as a result of the reaction between acidic species (mainly $HNO_3$) and NaCl, which produces sodium salts (mainly $NaNO_3$) and releases gas-phase HCl (EPA, 2004; Braun et al., 2017). As during the warm months the concentration of ammonium chloride is generally negligible, the summer distribution of chloride was unimodal.

A unimodal distribution almost completely confined in the coarse fraction, with maximum in the range 3.2 – 5.6 μm, was found for $Ca^{++}$, in agreement with the main source of this ion, originating from soil dust.

During winter, ammonium, nitrate and sulphate ions showed overlapping size distributions, almost exclusively in the fine fraction (maxima in the range 0.56 – 1.0 μm), in agreement with the secondary formation of ammonium nitrate and ammonium sulphate. During the summer period, instead, the concentration of ammonium nitrate severely decreased, as observed in the case of ammonium chloride, and the size distribution of nitrate became bimodal, with a prevailing contribution in the coarse fraction and maximum in the range 3.2 – 5.6 μm. This latter contribution was probably due to soil dust and to the products of the above cited reaction between $HNO_3$ and NaCl. $NH_4^{+}$ and $SO_4^{=}$ showed the same size distribution also during summer, in agreement with the photochemical formation of ammonium sulphate. It is worth noting that during summer the peak in the size distribution of sulphate was in the range 0.32 – 0.56 μm, while it was in the range 0.56 – 1.0 μm during winter. This constitutes a first indication of the effect due to the ageing of the air masses, which is of longer duration during the cold months.

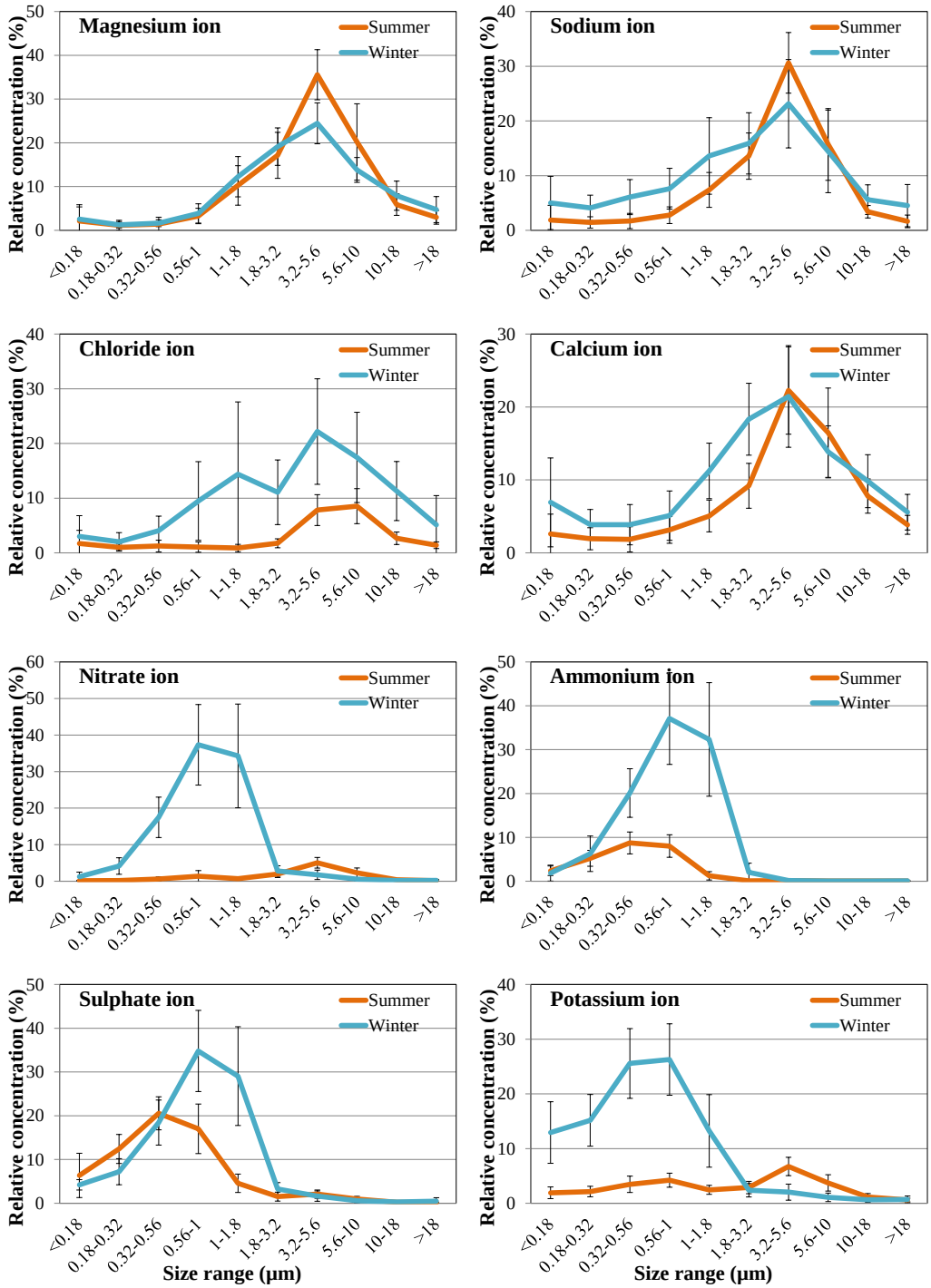


Figure 2: Size distribution of ions during summer (orange line) and winter (blue line); mean values and standard deviation of all the values recorded during the study.

In the case of $K^+$, remarkable winter-summer differences were observed, due to the prevalence of different sources: during summer this species is mainly released from the soil and showed a maximum in the coarse range 3.2 – 5.6 µm, as in the case of $Ca^{++}$; during winter, instead, the release from biomass burning largely prevails and the size distribution of $K^+$ was almost completely in the

fine fraction, with a broad maximum in the size range 0.32 – 1.0 μm. A similar size distribution was attributed to a relevant contribution of wood burning also in other studies (Ma et al., 2019).

Figure 3 reports the size distribution of the extracted ($_{ext}$) and residual ($_{res}$) fractions of Rb, Li e Cs. All three elements showed noticeable differences in the size distribution of the two solubility fractions. The soluble fraction populated almost exclusively the fine fraction of PM, while the residual fraction was found mostly in coarse particles. A similar behaviour was observed for the majority of the considered elements. These substantial differences in the size distribution of the two solubility fractions support the ability of the chemical fractionation method to differentiate PM sources (Canepari et al., 2008, 2009, 2014). The results in Figure 3 show that the concentration of $Rb_{ext}$, $Li_{ext}$ and $Cs_{ext}$ was much higher during winter than during summer, while the opposite pattern was observed in the case of $Rb_{res}$, $Li_{res}$ and $Cs_{res}$. The overlap of the size distributions and seasonal profiles supports the hypothesis of common sources, at least two, for these three elements. These sources could be identified in biomass burning for domestic heating during the winter period and in re-suspension of soil dust during the summer period. Biomass burning therefore affects mainly the soluble fraction of Rb, Li and Cs, while soil re-suspension impacts on their residual fraction.

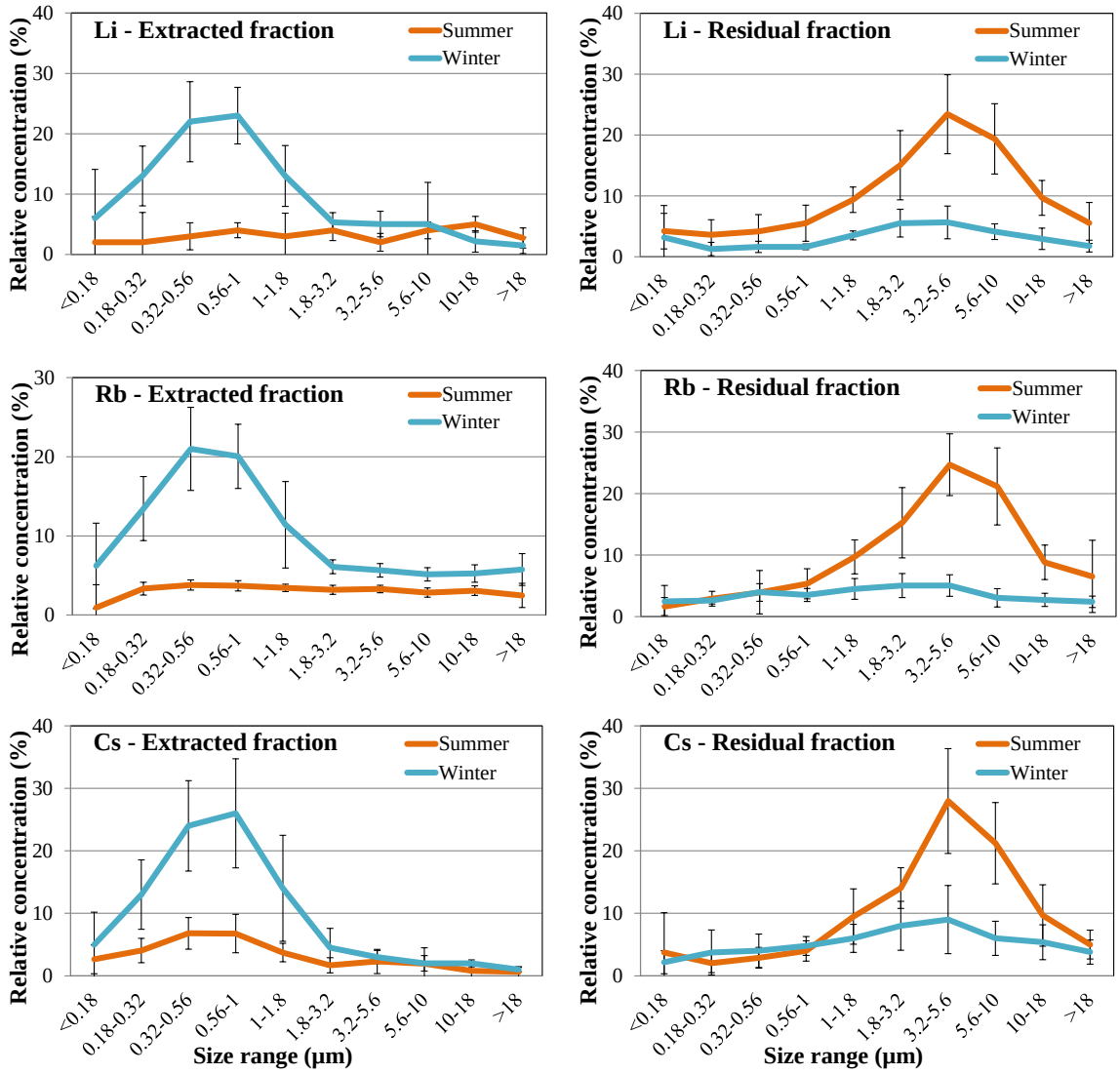


Figure 3: Size distribution of the extracted and residual fractions of Rb, Li and Cs; mean values and standard deviation of all the values recorded during the study.

It is interesting to note that the size distributions of $Rb_{ext}$, $Li_{ext}$ and $Cs_{ext}$ and their seasonal differences overlapped the results obtained for $K^+$, further confirming the existence of a common source. It should be noted that in the scientific literature $K^+$ is widely used as a tracer of biomass burning, while Rb, Li and Cs are not considered as reliable tracers of this source because the measurement of the total concentration, carried out in most studies, does not allow any distinction between the contributions of biomass burning and of soil (Vicente and Alves, 2018; Perrino et al., 2019).

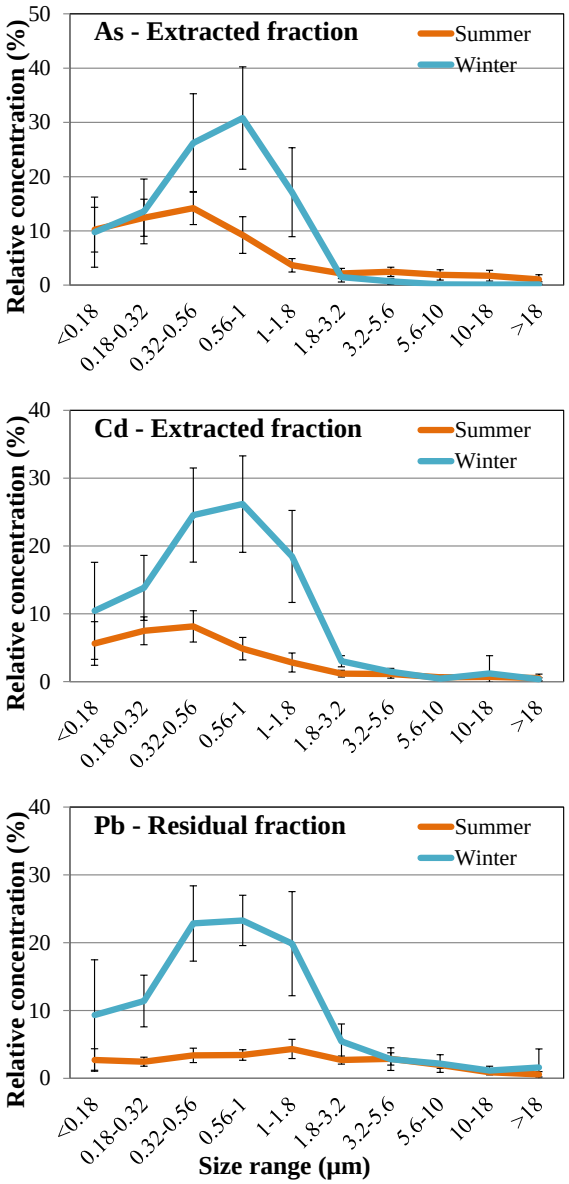


Figure 4: Size distribution of $As_{ext}$, $Cd_{ext}$, $Pb_{res}$;
mean values and standard deviation of all the values recorded during the study.

Figure 4 reports the size distribution of $As_{ext}$, $Cd_{ext}$, $Pb_{res}$, all elements regulated by the European legislation. Also in this case the fine fraction dominated the size distribution and the winter concentration exceeded summer values. Furthermore, their size distribution resembles those of $K^+$ and of the elements reported in the left column of Figure 3. This suggests that, during winter, biomass burning significantly contributed to the air concentration of these elements. The production of particles containing Pb in biomass combustion had been already reported in the literature (Vicente and Alves, 2018; Ma et al., 2019), while for As and Cd this link was less well-known. Also for these elements, adopting a chemical fractionation scheme and using the fraction that is more sensitive to

the considered source resulted in a considerable improvement of the selectivity of the element as a tracer.

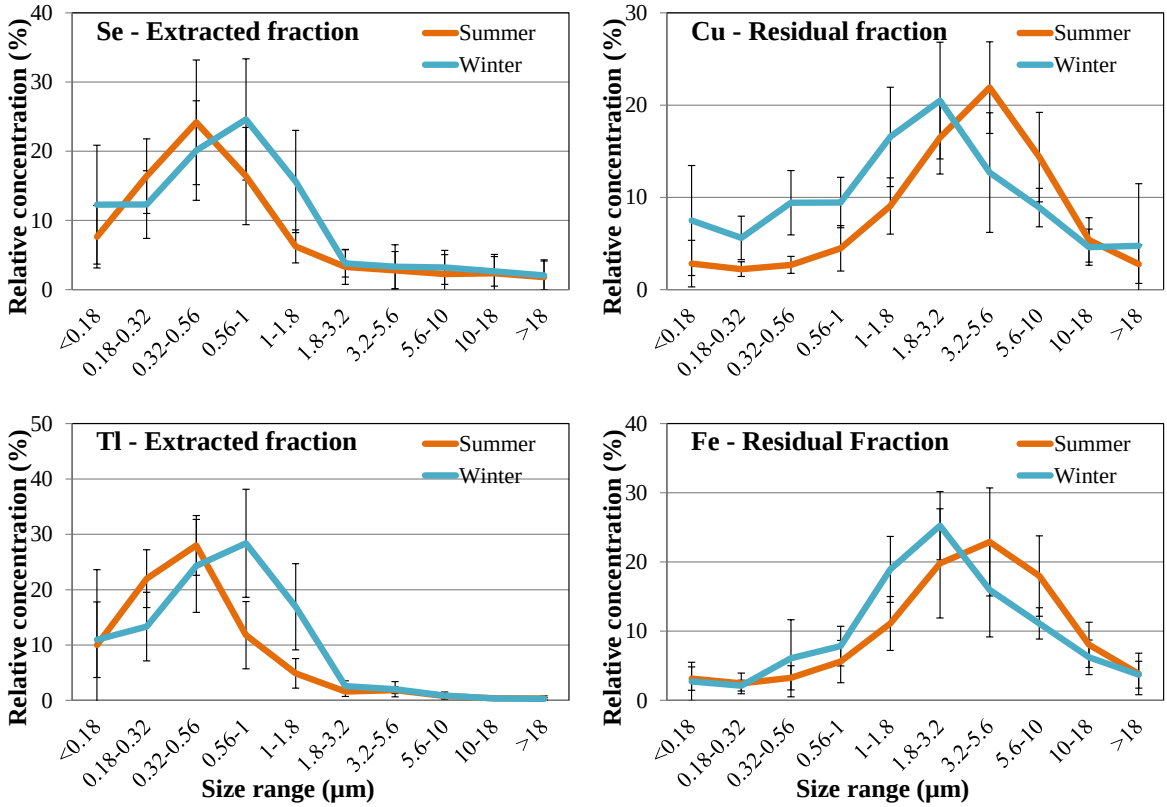


Figure 5: Size distribution of $Se_{ext}$, $Tl_{ext}$, $Fe_{res}$ and $Cu_{res}$;
mean values and standard deviation of all the values recorded during the study.

A similar behaviour, although less clear, is shown by some other elements: $Co_{ext}$, $Mn_{ext}$, $Sb_{ext}$, $Sn_{res}$ (Supplementary Material S3) and also in these cases it is reasonable to presume a non-negligible contribution of biomass burning. It is worth noting that most of these elements (Co, Sb, Sn) are generally considered as tracers of industrial sources (Farao et al., 2014; Ma et al., 2019). Nevertheless, the combined chemical/size fractionation approach allowed a reliable identification of the biomass burning contribution even in a heavily industrialized area.

$Se_{ext}$, $Tl_{ext}$, $Fe_{res}$ and $Cu_{res}$, instead, showed a size distribution characterised by small seasonal variations (Figure 5). This indicates that the strength of the PM sources containing these elements was quite constant during the year. These sources may be identified in the industrial plants for $Se_{ext}$ and $Tl_{ext}$, which were mostly found in the fine fraction of PM, and in the braking systems of vehicles, releasing particles in the coarse range, for $Fe_{res}$ and $Cu_{res}$ (Canepari et al., 2008; 2014).

However, we can notice a winter-summer difference in the size distribution of these elemental fractions. $Se_{ext}$ and $Tl_{ext}$, which were mainly in the fine fraction, show a shift in the size distribution towards higher values of the aerodynamic diameters during the winter, while in the case of $Fe_{res}$ and

$Cu_{res}$, mainly in the coarse fraction, the winter shift is towards lower values of the aerodynamic diameters. These variations can be explained considering that in winter atmospheric particles remain in the atmosphere for a much longer time than in summer. During ageing of the air masses, particles in the accumulation mode tend to increase their dimensions due to condensation/coagulation processes and water uptake, while particles in the coarse mode tend to decrease their dimensions because of the fall-off of the larger particles (EPA, 2004).

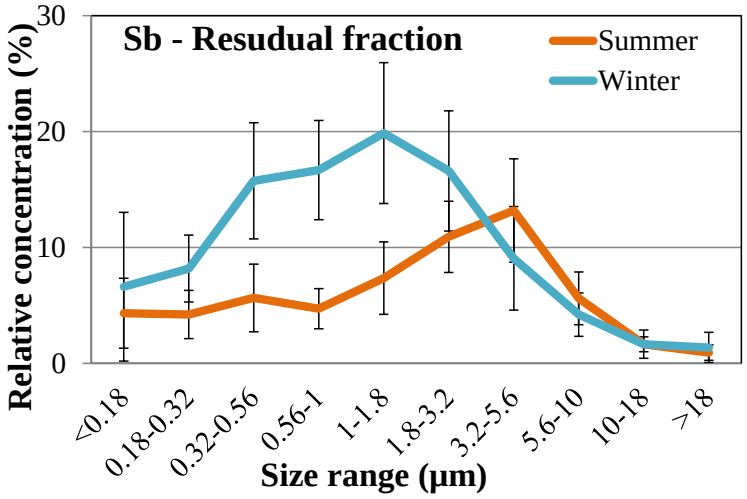


Figure 6: Size distribution of $Se_{res}$;
mean values and standard deviation of all the values recorded during the study.

Very interesting is the case of Sb, which is often used as a tracer of brake wear, together with Cu and Fe (Grigoratos and Martini, 2015). Previous studies carried out by applying the same chemical fractionation procedure used in this work, showed that the residual fraction is the solubility fraction that is most sensitive to this source (Canepari et al., 2008). During the warm period the size distribution of $Sb_{res}$, reported in Figure 6, overlapped the pattern of $Cu_{res}$ and $Fe_{res}$ (Figure 5), confirming the existence of a main common source. During winter, instead, the size distribution profile of $Sb_{res}$ differed from $Cu_{res}$ and $Fe_{res}$, suggesting the existence of two superimposed patterns due to different sources: one ascribable to brake wear, which contributed to the size fractions larger than 1.0 -1.8 µm, the other one responsible for a sharp increase in the size fractions below 1.8 µm and probably nameable as biomass burning.

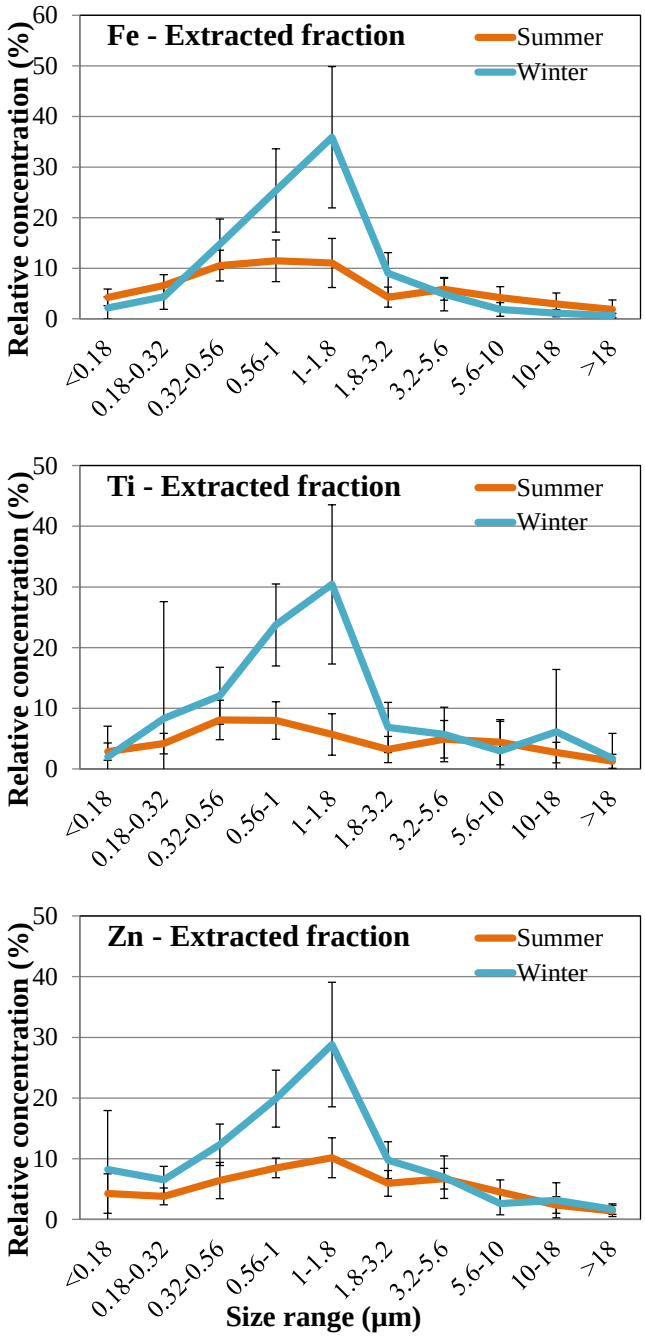


Figure 7: Size distribution of $Fe_{ext}$, $Ti_{ext}$ and $Zn_{res}$;
mean values and standard deviation of all the values recorded during the study.

The extracted fractions of Fe, Ti and Zn, shown in Figure 7, exhibited a still different behaviour. While the residual fractions of these elements, which were quantitatively prevailing, were distributed mainly the coarse fraction, $Fe_{ext}$,, $Ti_{ext}$, and $Zn_{ext}$ were almost completely found in the fine fraction of PM and shared the same winter distribution, with maxima in the size range 1.0-1.8 µm. Even if the contribution of the source of these elements increased during winter, the size distribution was different from that described for biomass burning. We may think that these tracers were released from

an industrial source that released fine particles and that was very far from the receptor. Therefore, in winter the particles produced by this source were long-range transported and, because of the atmospheric stability typical of the studied area, underwent ageing and dimensional increase. During the warm period PM was more easily diluted by convective mixing of the atmosphere and these particles might have not reached, or reached at a less extent, the receptor site.

## CONCLUSIONS

The study of a high number (41) of size-segregated samples collected during 7 years in a complex area such as the Po Valley allowed an in-depth study of the size distribution of ions and elements in atmospheric PM during the winter and the summer seasons.

The results of this study confirmed the typical size distribution of ions (mainly coarse for Na+, $Cl^-$, $Mg^{++}$ and $Ca^{++}$, mainly fine for $NO_3^-$, $SO_4^=$, $NH_4^+$ and $K^+$) and the very high concentrations of ammonium nitrate during the winter season.

The combination of the size fractionation with the elemental fractionation allowed us to draw interesting information about the reliability of some elements as source tracers. We identified the extracted fraction of Rb, Cs and Li as good and selective tracers of biomass burning, and observed that some other elements show a partial contribution from the same source ($As_{ext}$, Cd, $Pb_{res}$, $Sb_{res}$, Mn, $Co_{ext}$, Sn). This group includes some toxic elements, highlighting, once more, the potential danger to human health due to the emission from biomass burning for domestic heating.

For some elements released in the atmosphere from non-seasonal PM sources ($Cu_{res}$, $Fe_{res}$, $Se_{ext}$, $Tl_{ext}$) it was possible to observe an increase in the dimensions of fine particles during winter and a decrease in the dimension of coarse particles during summer, both ascribed to air mass ageing.

## AKNOWLEDGEMENTS

The Authors are indebted to S. Dalla Torre, T. Sargolini and S. Pareti for technical assistance during the sampling and the analytical phases of this work.

## REFERENCES

Arhami, M., Hosseini, V., Shahne, M. Z., Bigdeli, M., Lai, A., Schauer, J. J. (2017). Seasonal trends, chemical speciation and source apportionment of fine PM in Tehran. Atmospheric Environment, 153, 70-82.

Barbaro, E., Feltracco, M., Cesari, D., Padoan, S., Zangrando, R., Contini, D., Barbante, C., Gambaro, A. (2019). Characterization of the water soluble fraction in ultrafine, fine, and coarse atmospheric aerosol. Science of The Total Environment, 658, 1423-1439.

Bernardoni, V., Elser, M., Valli, G., Valentini, S., Bigi, A., Fermo, P., Piazzalunga, A., Vecchi, R. (2017). Size-segregated aerosol in a hot-spot pollution urban area: Chemical composition and three-way source apportionment. Environmental Pollution, 231, 601-611.

Bigi, A., Ghermandi, G. (2014). Long-term trend and variability of atmospheric PM 10 concentration in the Po Valley. Atmospheric Chemistry and Physics, 14(10), 4895-4907.

Braun, R. A., Dadashazar, H., MacDonald, A. B., Aldhaif, A. M., Maudlin, L. C., Crosbie, E., Aghdam, M.A., Mardi, A.H., Sorooshian, A. (2017). Impact of wildfire emissions on chloride and bromide depletion in marine aerosol particles. Environmental science & technology, 51(16), 9013-9021.

Canepari, S., Perrino, C., Olivieri, F., Astolfi, M.L. (2008). Characterisation of the traffic sources of PM through size-segregated sampling, sequential leaching and ICP analysis. Atmospheric Environment, 42, 8161-8175.

Canepari, S., Pietrodangelo, A., Perrino, C., Astolfi, M. L., Marzo, M. L. (2009). Enhancement of source traceability of atmospheric PM by elemental chemical fractionation. Atmospheric Environment, 43(31), 4754-4765.

Canepari, S., Perrino, C., Astolfi, M. L., Catrambone, M., Perret, D. (2009b). Determination of soluble ions and elements in ambient air suspended particulate matter: inter-technique comparison of XRF, IC and ICP for sample-by-sample quality control. Talanta, 77(5), 1821-1829.

Canepari, S., Astolfi, M. L., Moretti, S., Curini, R. (2010). Comparison of extracting solutions for elemental fractionation in airborne particulate matter. Talanta, 82(2), 834-844.

Canepari, S., Astolfi, M. L., Farao, C., Maretto, M., Frasca, D., Marcoccia, M., Perrino, C. (2014). Seasonal variations in the chemical composition of particulate matter: a case study in the Po Valley. Part II: concentration and solubility of micro-and trace-elements. Environmental Science and Pollution Research, 21(6), 4010-4022.

Cassee, F. R., Héroux, M. E., Gerlofs-Nijland, M. E., Kelly, F. J. (2013). Particulate matter beyond mass: recent health evidence on the role of fractions, chemical constituents and sources of emission. Inhalation Toxicology, 25(14), 802-812.

Castro, T., Peralta, O., Salcedo, D., Santos, J., Saavedra, M. I., Espinoza, M. L., Salcido, a., Celada-Murillo, A.T., Carreon-Sierra, S., Alvarez-Ospina, H., Carabali, G., Barrera, V, Madronich, S. (2018). Water-soluble inorganic ions of size-differentiated atmospheric particles from a suburban site of Mexico City. Journal of Atmospheric Chemistry, 75(2), 155-169.

Chrysikou, L. P., Samara, C. A. (2009). Seasonal variation of the size distribution of urban particulate matter and associated organic pollutants in the ambient air. Atmospheric Environment, 43(30), 4557-4569.

EPA. Air Quality Criteria for Particulate Matter (Final Report, 2004). U.S. Environmental Protection Agency, Washington, DC, EPA 600/P-99/002aF-bF, 2004.

Farao, C., Canepari, S., Perrino, C., Harrison, R. M. (2014). Sources of PM in an industrial area: comparison between receptor model results and semiempirical calculations of source contributions. Aerosol and Air Quality Research, 14(6), 1558-1572.

Gao, Y., Lee, S. C., Huang, Y., Chow, J. C., Watson, J. G. (2016). Chemical characterization and source apportionment of size-resolved particles in Hong Kong sub-urban area. Atmospheric Research, 170, 112-122.

Giorio, C., Tapparo, A., Scapellato, M. L., Carrieri, M., Apostoli, P., Bartolucci, G. B. (2013). Field comparison of a personal cascade impactor sampler, an optical particle counter and CEN-EU standard methods for PM10, PM2. 5 and PM1 measurement in urban environment. Journal of Aerosol Science, 65, 111-120.

Grigoratos, T., Martini, G. (2015). Brake wear particle emissions: a review. Environmental Science and Pollution Research, 22(4), 2491-2504.

Hwang, S. L., Chi, M. C., Guo, S. E., Lin, Y. C., Chou, C. T., Lin, C. M. (2018). Seasonal variation and source apportionment of PM 2.5-bound trace elements at a coastal area in southwestern Taiwan. Environmental Science and Pollution Research, 25(9), 9101-9113.

Kulshrestha, A., Satsangi, P. G., Masih, J., Taneja, A. (2009). Metal concentration of PM2. 5 and PM10 particles and seasonal variations in urban and rural environment of Agra, India. Science of the Total Environment, 407(24), 6196-6204.

Liu, X., Zhai, Y., Zhu, Y., Liu, Y., Chen, H., Li, P., Peng, C., Xu, B:, Li, C., Zeng, G. (2015). Mass concentration and health risk assessment of heavy metals in size-segregated airborne particulate matter in Changsha. Science of the Total Environment, 517, 215-221.

Ma, L., Dadashazar, H., Braun, R. A., MacDonald, A. B., Aghdam, M. A., Maudlin, L. C., Sorooshian, A. (2019). Size-resolved Characteristics of Water-Soluble Particulate Elements in a Coastal Area: Source Identification, Influence of Wildfires, and Diurnal Variability. Atmospheric Environment, 206, 72-84.

Marcazzan, G. M., Valli, G., Vecchi, R. (2002). Factors influencing mass concentration and chemical composition of fine aerosols during a PM high pollution episode. Science of the Total Environment, 298(1-3), 65-79.

Maudlin, L. C., Wang, Z., Jonsson, H. H., Sorooshian, A. (2015). Impact of wildfires on size-resolved aerosol composition at a coastal California site. Atmospheric Environment, 119, 59-68.

Nirmalkar, J., Deshmukh, D. K., Deb, M. K., Chandrawanshi, S., & Tiwari, S. (2016). Seasonal size distribution and possible health implications of atmospheric aerosols collected from a rural site of eastern central India. Atmospheric Pollution Research, 7(2), 278-287.

Pernigotti, D., Georgieva, E., Thunis, P., Bessagnet, B. (2012). Impact of meteorology on air quality modeling over the Po valley in northern Italy. Atmospheric Environment, 51, 303-310.

Perrino, C., Catrambone, M., Dalla Torre, S., Rantica, E., Sargolini, T., Canepari, S. (2014). Seasonal variations in the chemical composition of particulate matter: a case study in the Po Valley. Part I: macro-components and mass closure. Environmental Science and Pollution Research, 21(6), 3999-4009.

Perrino, C., Catrambone, M., Farao, C., Canepari, S. (2016). Assessing the contribution of water to the mass closure of PM10. Atmospheric Environment, 140, 555-564.

Perrino, C., Tofful, L., Dalla Torre, S., Sargolini, T., Canepari, S. (2019). Biomass burning contribution to PM10 concentration in Rome (Italy): Seasonal, daily and two-hourly variations. Chemosphere, 222, 839-848.

Salma I., Ocskay R., Raes N., Maenhaut W. (2005) Fine structure of mass size distributions in an urban environment. Atmospheric Environment, 39,5363–5374.

Squizzato, S., Masiol, M., Innocente, E., Pecorari, E., Rampazzo, G., Pavoni, B. (2012). A procedure to assess local and long-range transport contributions to PM2. 5 and secondary inorganic aerosol. Journal of Aerosol Science, 46, 64-76.

Taiwo, A.M., Beddows, D.C.S., Shi, Z., Harrison, R.M. (2014). Mass and number size distribution of particulate matter components: Comparison of an industrial site and an urban background site. Science of the Total Environment, 475, 29-38.

Vicente, E. D., Alves, C. A. (2018). An overview of particulate emissions from residential biomass combustion. Atmospheric Research, 199, 159-185.

Wang, Q., Ma, Y., Tan, J., Zheng, N., Duan, J., Sun, Y., He, K., Zhang, Y. (2015). Characteristics of size-fractionated atmospheric metals and water-soluble metals in two typical episodes in Beijing. Atmospheric Environment, 119, 294-303.

Wang, J., Zhou, M., Liu, B. S., Wu, J. H., Peng, X., Zhang, Y. F., Han S.Q., Zhu, T. (2016). Characterization and source apportionment of size-segregated atmospheric particulate matter collected at ground level and from the urban canopy in Tianjin. Environmental Pollution, 219, 982-992.

Zhang, J., Tong, L., Huang, Z., Zhang, H., He, M., Dai, X., Zheng, J., Xiao, H. (2018). Seasonal variation and size distributions of water-soluble inorganic ions and carbonaceous aerosols at a coastal site in Ningbo, China. Science of The Total Environment, 639, 793-803.

387